SKIN HEMOGLOBIN AND MELANIN QUANTIFICATION ON MULTI-SPECTRAL IMAGES

Hao GONG
GIPSA-Lab
Grenoble Institute of Technology
Domaine Universitaire, BP 46, 38402
Grenoble, France
hao.gong@gipsa-lab.grenoble-inp.fr

Michel DESVIGNES
GIPSA-Lab
Grenoble Institute of Technology
Domaine Universitaire, BP 46, 38402
Grenoble, France
michel.desvignes@gipsa-lab.grenoble-inp.fr

ABSTRACT

In this paper, we propose and compare two different approaches for quantification of skin hemoglobin and melanin on multi-spectral images. The first method is based on non-negative matrix factorization (NMF) with multiplicative update algorithm. The second method is a Beer-Lambert law based model-fitting technique. Quantitative evaluation through graph-cut segmentation on melanoma indicates that model-fitting method obtains more accurate quantification than NMF.

KEY WORDS

multi-spectral images, hemoglobin, melanin, NMF, model-fitting, graph cuts.

1 Introduction

An accurate quantification of skin pigmentation is of primary importance for the objective diagnosis and grading of skin diseases. In this paper, we propose to use multi-spectral images to quantify skin hemoglobin and melanin. The interest of working with multi-spectral images is to have more accurate information on skin properties than those obtained on conventional cameras. Several methods based on spectrum in visible wavelength range have already been presented in the literature[1][2]. The main idea of these methods is to select specific spectral bands in the data to extract information on skin pigmentation.

In this paper, we propose to extract hemoglobin and melanin components considering the whole spectrum. Multi-spectral images acquired in visible wavelength region (e.g. 400-700 nm) are input into a mathematical optical skin model that considers the contributions from different chromophores in the epidermis and dermis skin layers. Through two different algorithms, non-negative factorization and least-squares based model fitting, we can quantify the concentrations of hemoglobin and melanin in a given area of skin lesion and surrounding heathy skin. To evaluate quantitatively, we apply graph-cut segmentation to both inputs and outputs of the proposed algorithms. Experimental results indicate that model-fitting approach obtains more accurate quantitative estimation than NMF.

2 Materials and Methods

2.1 Multi-spectral Image Acquistion

The multi-spectral imaging system (*SpectraCam*TM, Newtone Technologies, Lyon, France) used in this work contains a liquid crystal tunable filter (LCTF) (VariSpecTM, Model VIS2, Cambridge Research & Instrumentation, Inc., Boston, MA) fitted in front of a PCO SensiCam Model 370 KL camera with 1168×1036 pixels on a progressive scan CCD image sensor (PCO Computer Optics, 93309 Kelheim, Germany) and a linear polarizing filter. The LCTF has a nominal bandwidth of 30 nm and a nominal accuracy of the selected peak wavelength of 4 nm. This allows to select about 80 significantly different tuning positions in the range from 400 nm to 720 nm. A linearly polarized light source was used with its polarization plane positioned vertical to the polarization plane of the camera polarizer. Thus, artifacts due to specular reflection were eliminated.

The multi-spectral images were acquired over the whole melanoma area and the surrounding healthy skin in the wavelength range 400-700 nm with the scanning step 10 nm. Inhomogeneities of illumination were removed by normalizing the acquired multi-spectral images with corresponding ones of white reflectance standard.

2.2 Model of Skin Optics

Fig.1 shows the schematic model of imaging process of three layered model of skin. Two predominant chromophores found in epidermal and dermal layers are melanin and hemoglobin[3]. Based on Beer-Lambert law, the absorbance of this skin model at a wavelength $\lambda(A(\lambda))$ can be expressed as

$$\begin{aligned} A(\lambda) &= \log(1/R(\lambda)) \\ &= \epsilon_{\text{Hb}}(\lambda)l_{\text{Hb}}(\lambda)c_{\text{Hb}} + \epsilon_{\text{Mel}}(\lambda)l_{\text{Mel}}(\lambda)c_{\text{Mel}} \end{aligned} \quad (1)$$

where R is the reflectance of the skin, l is the light penetration depth, c denotes the concentration of the chromophore and ϵ is the extinction coefficient that depends on absorbance spectrum of the chromophore (as shown in Fig.2 plotted in logarithmic scale).
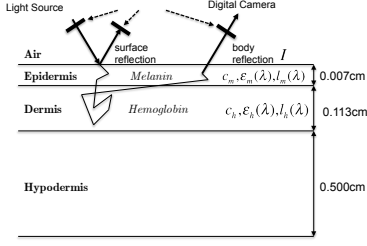
Figure 1. Three-layered skin model.

The extinction coefficient of hemoglobin has local maxima between 542 nm and 577 nm, which provides a convenient wavelength region for the quantification of hemoglobin. The extinction coefficient of melanin has no characteristic maximum in the visible region but demonstrates a monotonic decrease towards larger wavelengths. Particularly, in red region of the spectrum (> 600 nm), the molar absorptivity of melanin is more prominent compared with the other chromophore. Hence, the red region can be used for melanin quantification.
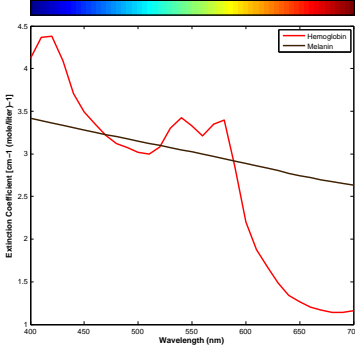

Figure 2. Molar absorptivity spectra of chromophores.

2.3 Erythema Index and Melanin Index

Erythema index (EI) and melanin index (MI) hold excellent linearity with hemoglobin concentration and melanin concentration respectively. Unlike color coordinates such as $L^*a^*b^*$, the EI and MI are not indicators for evaluating 'color' but represent an index for quantifying the amounts of hemoglobin and melanin. Based on the theories of absorbance of skin model (Section 2.2), Takiwaki et al.[2] proposed a simple method to derive EI and MI images from multi-spectral images. The equations for calculating EI and MI are written as follows:

$$EI = \log_{10}(1/\boldsymbol{R}_{\lambda_1}) - \log_{10}(1/\boldsymbol{R}_{\lambda_2}) \quad (2)$$
$$MI = \log_{10}(1/\boldsymbol{R}_{\lambda_2}) \quad (3)$$

where $\boldsymbol{R}_\lambda = \boldsymbol{S}_\lambda/W_\lambda$. $\boldsymbol{R}_\lambda$ is the normalized reflectance image of the sample under study, $\boldsymbol{S}_\lambda$ is the acquired image

of the sample and W_λ is the white standard. λ_1 is set at a wavelength range of 540-570nm, and λ_2 is at 620-650nm. In fact, this method is a simplified application of algorithm proposed by Stamatas[1] within visible spectrum range.

2.4 Non-negative Matrix Factorization Based Approach

Non-negative matrix factorization (NMF) suggested by Lee and Seung[4] is a useful method of decomposition of multivariate data. The method explicitly enforces the nonnegativity constraint on the values of the source data as well as the mixing quantities of the source data forming the mixed data. Compared to other source separation method like ICA, NMF has two main advantages in application to our problem. First, non-negativity constraint on the source data prevents meaningless negative value of chromophore concentration. Second, no constrain on the orthogonality of the source data allows dependency between skin chromophores, which is closer to the reality. The problem of source separation can be formulated as a linear mixture separation problem as in (4).

$$\boldsymbol{X} = \boldsymbol{AS} \quad (4)$$

where $\boldsymbol{X}$ is the observation data matrix of m rows and n columns, with each row representing the absorbance image vector at each wavelength. $\boldsymbol{S}$ is a source data matrix of l rows and n columns, with l being the number of sources to be extracted. The matrix $\boldsymbol{A}$ is known as the mixing matrix with m rows and l columns. The columns of which represent the mixing values of each source component. According to the absorbance of the multi-layered model described in Section 2.2. Equation (1) can be modified in form of Equation (4):

$$\begin{bmatrix} \log(1/\boldsymbol{r}(\lambda_1)) \\ \vdots \\ \log(1/\boldsymbol{r}(\lambda_m)) \end{bmatrix}_{m \times n} = \begin{bmatrix} \epsilon_h(\lambda_1) & \epsilon_m(\lambda_1) \\ \vdots & \vdots \\ \epsilon_h(\lambda_m) & \epsilon_m(\lambda_m) \end{bmatrix}_{m \times 2} \begin{bmatrix} \boldsymbol{c}_h \\ \boldsymbol{c}_m \end{bmatrix}_{2 \times n} \quad (5)$$

where $\boldsymbol{r}(\lambda_i)$ is the normalized reflectance image at wavelength λ_i. $\epsilon_{h,m}(\lambda_i)$ are extinction coefficients of hemoglobin and melanin at wavelength λ_i, respectively. $\boldsymbol{c}_{h,m}$ denote concentration distribution maps of hemoglobin and melanin. The non-negativity constraint is enforced on the source data and the mixing matrix as $\boldsymbol{S} \geq 0$ and $\boldsymbol{A} \geq 0$ respectively. Therefore, the problem can be formulated as a maximum-likelihood problem with least squares solution as in (6).

$$\boldsymbol{A}_{ML}, \boldsymbol{S}_{ML} = \arg\max_{\boldsymbol{A}, \boldsymbol{S}} p(\boldsymbol{X}|\boldsymbol{A}, \boldsymbol{S}) \quad (6)$$
$$\Rightarrow F = \arg\min_{\boldsymbol{A}, \boldsymbol{S}} \|\boldsymbol{X} - \boldsymbol{AS}\|^2 \quad (7)$$
$$Subject\ to : \boldsymbol{A} \geq 0, \boldsymbol{S} \geq 0$$

In the maximum likelihood optimization, the negative loglikelihood of F is minimized i.e. $\log\|\boldsymbol{X} - \boldsymbol{AS}\|$ is computed at each iteration. Here, $\|\cdot\|$ is the Euclidean norm.

The updates of A and S can be performed under the 'multiplicative update rule' in forms as (8).

$$A \leftarrow A \frac{XS^\top}{ASS^\top}, \quad S \leftarrow S \frac{A^\top X}{A^\top AS} \qquad (8)$$

This rule ensures the non-negative properties of the optimal solutions, A_{ML} and S_{ML} if the initial matrices A_{initial} and S_{initial} are strictly positive. The initialization of the source data matrix S is given by EI and MI and the mixing matrix A can be initialized using least squares estimation with a single constraint as given in (10).

$$S_{\text{initial}} = \begin{bmatrix} EI \\ MI \end{bmatrix} \qquad (9)$$

$$\underset{A_{\text{initial}}}{\arg\min} \|X - A_{\text{initial}}S_{\text{initial}}\|^2 \qquad (10)$$
$$Subject\ to : A_{\text{initial}} \geq 0$$

The dimension m is 26 in our experiment since we use multi-spectral images over 26 wavelengths sampled between 450-700nm.

2.5 Model-Fitting Based Approach

Source separation based approaches, like ICA and NMF, give us a statistical tool to quantify skin hemoglobin and melanin in case that the mixing matrix A is unknown.

In this section, we employ a more accurate model which includes oxy-hemoglobin and deoxy-hemoglobin based on the oxygen-saturation of hemoglobin. So that Equation (4) can be rewritten as

$$\begin{bmatrix} \log(1/r(\lambda_1)) \\ \vdots \\ \log(1/r(\lambda_m)) \end{bmatrix} = \begin{bmatrix} \epsilon_{hO2}(\lambda_1) & \epsilon_h(\lambda_1) & \epsilon_m(\lambda_1) \\ \vdots & \vdots & \vdots \\ \epsilon_{hO2}(\lambda_m) & \epsilon_h(\lambda_m) & \epsilon_m(\lambda_m) \end{bmatrix} \begin{bmatrix} c_{hO2} \\ c_h \\ c_m \end{bmatrix} \qquad (11)$$

where the mixing matrix A is approximated using tabulated extinction coefficients of three predominant chromophores[5][6], $\epsilon_{hO2}(\lambda_i)$, $\epsilon_h(\lambda_i)$ and $\epsilon_m(\lambda_i)$ at wavelength λ_i. Now the problem is simply to fit this model by solving a system of linear equations. Solutions of this overdetermined system can be obtained using least-squares estimation with a single constraint as given in (12).

$$\underset{A_{\text{tabulated}}}{\arg\min} \|X - A_{\text{tabulated}}S\|^2 \qquad (12)$$
$$Subject\ to : S \geq 0$$

3 Results and Discussion

In this section, we compare the proposed algorithms using acquired multi-spectral images of melanoma at 26 wavelength sampled equally from 450 nm to 700 nm. Based on the dermatologic knowledge that (i) vasculature contains higher concentration of hemoglobin and lower concentration of melanin, (ii) increase of melanin content and decrease of hemoglobin content are responsible for the dark color of melanoma, one can see that model-fitting method

outperforms NMF based method in extracting relatively accurate concentration cartographies of hemoglobin and melanin. For example, NMF based method overestimates the hemoglobin concentration within the central melanoma area (Fig.3(b)) and underestimates the melanin concentration on the near-border melanoma area (Fig.3(c)).

(a) Reconstructed Color Image

(b) Hemoglobin by NMF   (c) Melanin by NMF

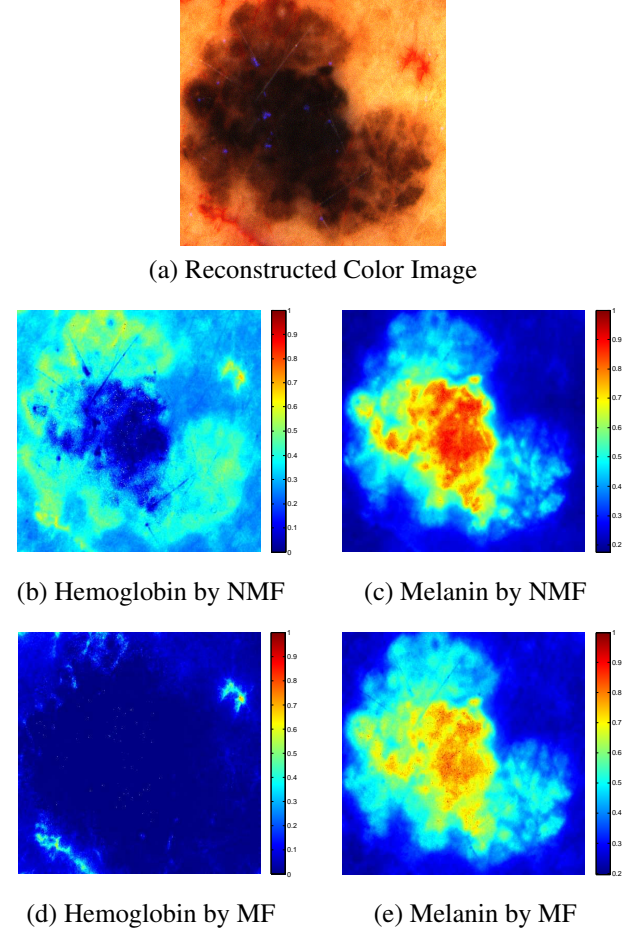(d) Hemoglobin by MF   (e) Melanin by MF

Figure 3. Comparison of hemoglobin and melanin concentration cartographies on 'Melanoma'. 'MF': model-fitting method.

In context of melanoma detection, a precise and robust segmentation of skin pigmented lesion is required to discriminate tumor cell boundary and the surrounding tissue. Thus, the accuracy of the different quantification methods can be evaluated by the accuracy of the segmentation of melanoma, measured by Dice similarity coefficient (DSC), false negative ratio (FNR) and false positive ratio (FPR). We use extracted melanin images (Fig. 3(c),(e)) as well as the 26 acquired multi-spectral images to perform the graph-cut segmentation. The manual input seed map (Fig.4(a)) and the manual segmented ground truth (Fig.4(b)) are both obtained from dermatologists. First, we compare a classic graph-cut segmentation on reconstructed color image (Fig.3(a)) with a modified approach on and 26-level images (26 multi-spectral images). It will

be demonstrated below that using multi-spectral images, performance of segmentation can be enhanced considerably. Second, we compare the segmentation results on 4-level images (reconstructed color image + melanin image) with 27-level images (multi-spectral images + melanin image). In Table 2, we can observe that how model-fitting method achieves better results compared with NMF based method. The DSC is increased to 0.965 while both FNR and FPR decrease.
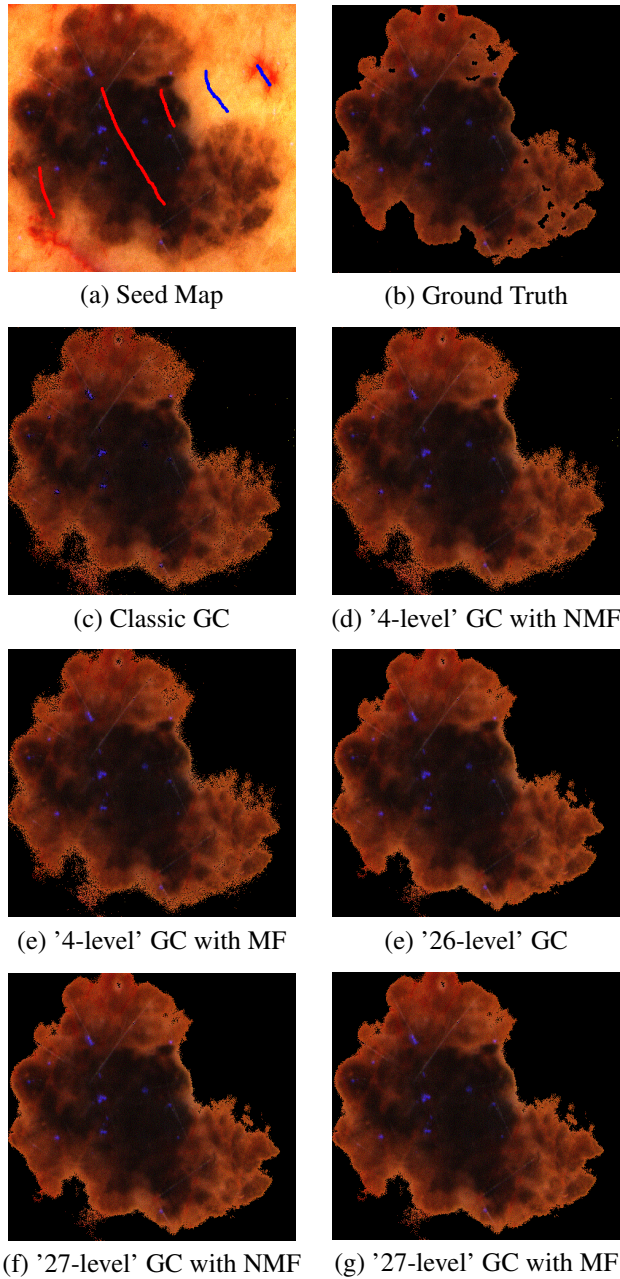
Table 1. Comparison of Segmentation Accuracy (Part 1)

	4-level MF	4-level NMF	Classic GC
DSC	0.954	0.950	0.943
FNR	0.009	0.011	0.026
FPR	0.085	0.092	0.091

Table 2. Comparison of Segmentation Accuracy (Part 2)

	27-level MF	27-level NMF	26-level GC
DSC	0.965	0.963	0.962
FNR	0.008	0.008	0.008
FPR	0.065	0.067	0.068

4   Conclusions

In this paper, we propose and compare two different quantitative estimation approaches on multi-spectral skin images using NMF and model fitting. By means of two comparative experiments based on dermatologic knowledge and graph-cut segmentation, we show that model-fitting approach obtains more accurate quantitative estimation of skin hemoglobin and melanin. In future work, scattering and penetration depth will be taken into account in skin optics model.

References

[1] Stamatas, G.N., Zmudzka, B.Z., Kollias N.: Non-invasive measurements of skin pigmentation in situ. Pigment Cell Research, vol. 17, pp. 618–626 (2004)

[2] Yamamoto, T., Takiwaki, H., Ohshima, H.: Derivation and clinical application of special imaging by means of digital cameras and imagej freeware for quantification of erythema and pigmentation. Skin Research and Technology, vol. 14, pp. 26–34 (2008)

[3] Anderson, R.R., Parrish, J.A.: The optics of human skin. J. Investig. Dermatol, vol. 77, pp. 13–19 (1981)

[4] Lee, D.D., Seung, H.S.: Learning the parts of objects by non-negative matrix factorization learning the parts of objects by non-negative matrix factorization. Nature, vol. 401, pp. 788–791 (1999)

[5] Prahl, S.: Tabulated molar extinction coefficient for hemoglobin in water, `http://omlc.ogi.edu/spectra/hemoglobin/summary.html`

[6] Jacques, S.: Extinction coefficient of melanin, `http://omlc.ogi.edu/spectra/melanin/eumelanin.html`

(a) Seed Map
(b) Ground Truth
(c) Classic GC
(d) '4-level' GC with NMF
(e) '4-level' GC with MF
(e) '26-level' GC
(f) '27-level' GC with NMF
(g) '27-level' GC with MF

Figure 4.   Comparison of segmentation results on 'melanoma'. 'GC': graph-cut.